T.3: Studies on Yb-doped double-clad CW and pulsed fiber lasers

B.N.Upadhaya, Solid State Laser Division
email: bnand@rrcat.gov.in

High power laser generation using Yb-doped double-clad fibers with conversion efficiencies in excess of 80% [1] have attracted much attention recently due to their inherent advantages in terms of very high efficiency, no misalignment due to in-built intra-core fiber Bragg gratings, low thermal problems due to large surface to volume ratio, diffraction-limited beam quality, compactness, reliability and fiber optic beam delivery. Yb-doped fibers can provide a wide emission band from ~ 1010 nm to ~ 1170 nm, which makes it a versatile laser medium to realize continuous-wave (CW), Q-switched short pulse, and mode-locked ultra-short pulse generation for various applications. There are several reports on the generation of high power single transverse mode output using Yb-doped double-clad large mode area fibers [1,2]. However, in scaling output power to kilowatt level, issues related to doped fiber quality, pump coupling efficiency, optical cavity design and thermal management become important. In high power scaling, small core of the doped fiber is subjected to high peak power densities, which may lead to the onset of nonlinearities and catastrophic damage of the active fiber. Although the damage threshold for pure silica is about 10 GW/cm^2, it may have smaller values in the case of doped silica fibers. Fig.T.3.1 shows energy level diagram of Yb ion in silica fiber [3]

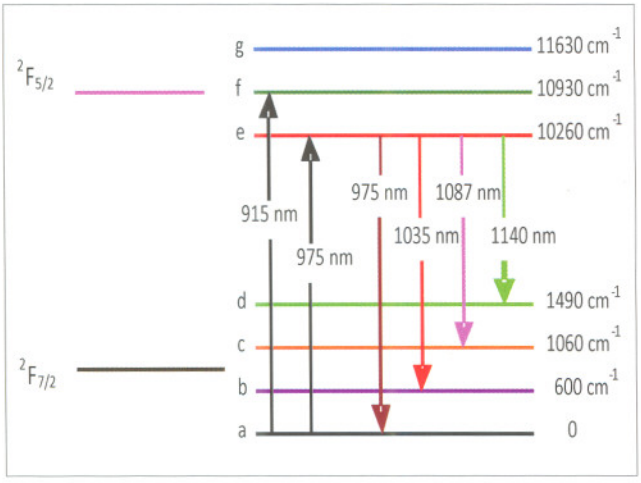

Fig. T.3.1: Energy level diagram of Yb ion in silica.

Yb possesses a simple atomic structure with only two principal manifolds i.e., ground level ($^2F_{7/2}$) and an excited state ($^2F_{5/2}$) separated by ~ 10000 cm^{-1}, which makes it an ideal rare-earth element for lasing. The three sublevels of the upper $^2F_{5/2}$ manifold are denoted as 'e', 'f', and 'g' and the four sublevels of the lower $^2F_{7/2}$ manifold are labeled as 'a', 'b', 'c', and 'd'. Weak multi-phonon decay is practically the only non-radiative channel that exists. The excited state has a lifetime of ~ 1 ms and acts as metastable level. The absence of higher energy levels near the upper manifold reduces the occurrence of multi-photon relaxation and excited state absorption (ESA). Yb ions are pumped into the sublevels of the $^2F_{5/2}$ manifold and laser emission results by transition from sublevel 'e' of $^2F_{5/2}$ manifold to sublevels 'a', 'b', 'c', and 'd' of $^2F^{7/2}$ manifold. Figure T.3.2 shows the absorption and emission cross-sections of Yb-doped Alumino-silicate glass. Pumping can, in principle, be done in a broad range from 900 nm to 1060 nm, while gain can be realized at the 975 nm peak or around the secondary peak starting from ~ 1020 nm to ~ 1150 nm. However, there are two main absorption peaks: one at 915 nm for excited state transition a →f and the other at 975 nm for transition a→ e. For pumping at 915 nm, lasing transition can occur from level e→ a at ~ 975 nm or from level e b, 'c', or 'd' in the range 1020-1150 nm. For pumping at 975 nm, lasing transition can occur from level e→b, 'c', or 'd' in the range 1020-1150 nm. For lasing transition below ~ 990 nm, it acts as a true three-level system and for lasing from ~ 1020 nm to ~ 1150 nm, it acts as a quasi four-level system.

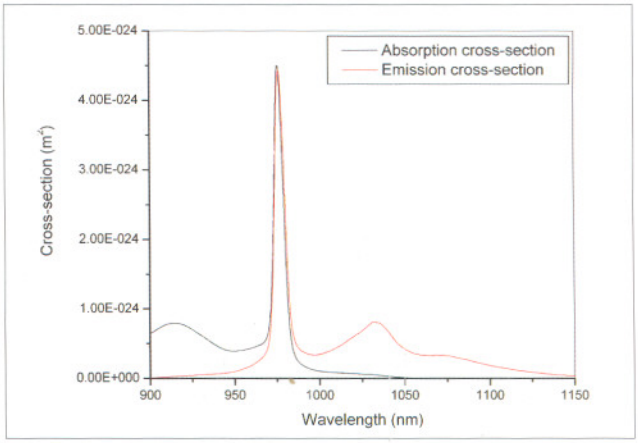

Fig.T.3.2: Absorption and emission cross-section of Yb-doped Alumino-silicate glass.

For high-power fiber lasers, low threshold is not of concern. In contrast to fiber communication systems where fibers are required to have small single-mode cores, small cores turn out to be an obstacle in the generation of high power laser outputs. Pumping of single-clad single-mode fiber requires single-mode laser-diode pump sources, and the output from single-mode pigtailed diodes is normally limited to below 1 W, hence the output from single-clad single-mode fiber lasers is also limited to below 1 W. The clad pumping technology using double-clad fiber structure was developed

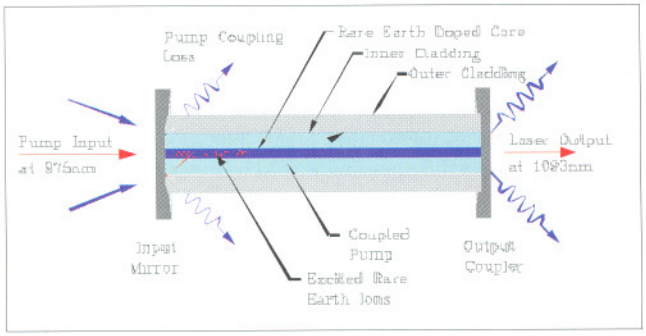

Fig.T.3.3 : Schematic of a double-clad fiber laser configuration.

as a solution for this limitation. A typical double-clad fiber is designed such that the core supports a large-area fundamental mode for efficient absorption of the pump; the inner cladding is of a larger diameter and high numerical aperture for efficient coupling from multimode diode bars. The shape of the inner cladding is normally non-circular in order to achieve better absorption of pump in the doped core region. Thus, cladding-pumped fiber lasers can be treated as devices to generate diffraction-limited single-mode laser output using multimode pump lasers. With large size inner cladding, very high pump powers can be launched into a double-clad fiber. However, the core size limits the output power to a certain level due to the onset of optical damage and thermal effects. Figure T.3.3 shows schematic of a double-clad fiber laser configuration.

CW fiber laser and self-pulsing dynamics:

High power CW Yb-doped fiber lasers with stable output power are of interest for various applications, such as pump source for other lasers and optical parametric oscillators, in spectroscopy and study of nonlinear phenomenon. However, it is not easy to achieve a truly CW fiber laser having stable output power (without fluctuations). Under CW pumping conditions, it is normally expected to have a CW output from fiber lasers. However, in several CW pumped rare-earth doped fiber lasers, for different resonator configurations and pumping geometries self-pulsation in the output has been reported [4,5]. Two types of self-pulsations in fiber lasers are reported in the literature: sustained self-pulsing (SSP) and self-mode locking (SML). SSP is the emission of high intensity pulses at irregular intervals, whereas SML refers to the laser output modulation or 'spiking' in the output with period corresponding to the cavity round-trip time. Several possible mechanisms such as ion-pairing acting as a saturable absorber, re-absorption of laser photons in the un-pumped part of the doped fiber, external perturbation such as pump noise, relaxation oscillations of the inversion and photon populations, interaction between laser signal and population inversion, distributed Rayleigh scattering, cascaded stimulated Brillouin scattering (SBS) and other nonlinear effects (stimulated Raman scattering (SRS), self-phase modulation (SPM), cross-phase modulation (XPM) and four-wave mixing (FWM)) as the sources of self-modulation and self-pulsing in different rare-earth doped fiber lasers have been reported [6,7]. Techniques to exploit self-pulsing to achieve regular narrow pulses with enhanced Q-switching have also been reported. There have also been substantial efforts to eliminate self-pulsing. The reported techniques to suppress self-pulsing include use of unidirectional fiber ring cavity, use of a low-transmission output coupler to realize a high Q-cavity, resonant pumping near the lasing wavelength to prevent rapid depletion of gain, thereby minimizing relaxation oscillations, electronic feedback to the pump laser to shift the gain and phase, increasing the cavity round-trip time by adding a long section of passive fiber to change the dynamics of relaxation oscillation, using fast saturable gain of a semiconductor optical amplifier within the fiber laser cavity, and use of the narrow pass-band of a λ/4-shifted FBG structure in a ring cavity to limit the number of longitudinal cavity modes [8,9]. Although there has been a considerable amount of effort to understand and control self-pulsing

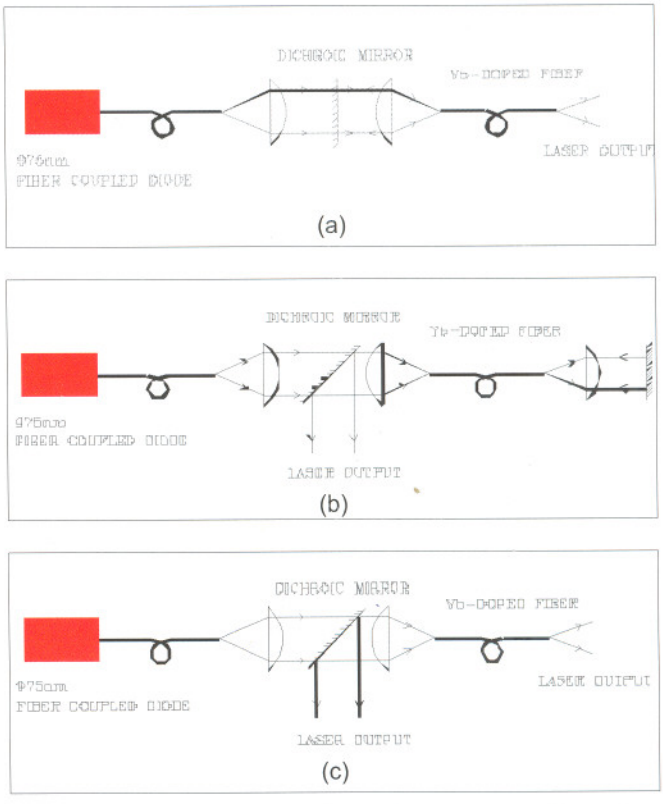

Fig.T.3.4 : (a) High-finesse forward pumping configuration in which output power is taken from the farther end. (b) High-finesse backward pumping configuration in which output power is taken from the pumping end using the tilted dichroic mirror. (c) Low-finesse resonator configuration.

phenomenon in fiber lasers, there is plenty of scope for research and in-depth understanding of the physical parameters responsible for this phenomenon.

For study of CW laser generation and self-pulsing dynamics, three different Fabry-Perot resonator configurations, shown in Fig. T.3.4a-c, were studied [10]. The experimental set up consisted of a Yb-doped double-clad fiber having a core diameter of 10 m with numerical aperture (NA) of 0.075, and an inner clad diameter of 400 m with a NA of 0.46. This Yb-doped fiber had an octagonal inner clad geometry and clad-pump absorption of 0.8 dB/m at 975 nm. A 20 W fiber-coupled laser diode with center wavelength 975 nm was used to pump 18 m length of the Yb-doped fiber. The pump laser output from the 200μm core fiber pigtail was collimated using a lens of 25 mm focal length and then focused using another lens of 25 mm focal length to image the pump fiber end on to the input end of the doped fiber. The doped fiber was cleaved at the ends to sustain higher damage thresholds.

Figure T.3.4(a) shows the high-finesse forward pumping configuration in which the dichroic mirror is kept in between the two lenses used for coupling pump light in to the doped fiber; the cleaved end with ~ 4% Fresnel reflection at the farther fiber end of the doped fiber acts as the output coupler. Figure T.3.4(b) shows the high-finesse backward pumping configuration in which two dichroic mirrors have been used; the cleaved end with ~ 4% Fresnel reflection from the pump input end of the doped fiber acts as the output coupler. Figure T.3.4(c) shows the low-finesse fiber laser resonator configuration, and in this case the cleaved ends with ~ 4% Fresnel reflection from both the fiber ends act as the Fabry-Perot cavity mirrors. The dichroic mirror used in these configurations is highly transmitting at 975nm and highly reflecting (~ 98%) in the wavelength range 1064-1140 nm. A maximum output power of 10.75 W was achieved at an input pump power of 17.2 W, with a slope efficiency of ~ 73% and an optical-to-optical conversion efficiency of 62.5%, in the backward pumping configuration. The laser output was in single transverse mode with diffraction-limited beam quality, and was emitted in a full cone angle of 150 mrad, defined by the NA of the doped fiber.

In the case of low-finesse resonator configuration, experimentally it was observed that the CW output power from both the ends ceases to increase beyond 1.8 W, and starts fluctuating due to occurrence of strong random self-pulsing. With further increase in the pump power, the peak power of these random pulses increased, and an increase in the fluctuation about the average output power was observed. Figure T.3.5(a) shows the observed random self-pulsing, and Fig. T.3.5(b) shows the expanded view of one of the random pulses with pulse duration less than 25 ns, for an input pump power of 8 W. As the pulses are random in time, and their peak-powers are not constant, the (measured) average power keeps fluctuating. Self-pulsing was also observed for high-finesse forward- and backward-pumping configurations, but the peak power of these self-pulses was very low as compared to that for low-finesse cavity, and a decrease in the peak power of these self-pulses occurred with increase in pump power. This is due to increase in gain uniformity along the fiber length with increase in pump power. Fig. T.3.6 shows the output spectrum before and after the onset of random self-pulsing. It shows the presence of nonlinear SRS and SBS effects with presence of first and second order Stokes lines shifted from the main laser line.

As the degree of non-uniformity of steady-state gain profile is different for high- and low-finesse cavities, these

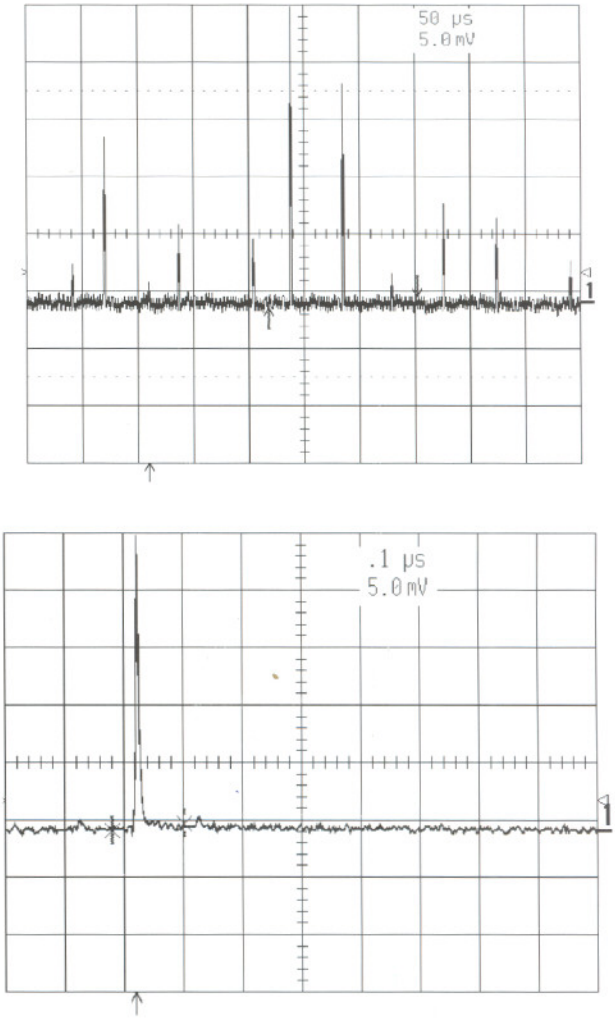

Fig.T.3.5 : (a) Output of the fiber laser, showing random self-pulses in the case of the low-finesse cavity, for an input pump power of 8 W. (b) An expanded oscilloscope trace of one of the random self-pulses.

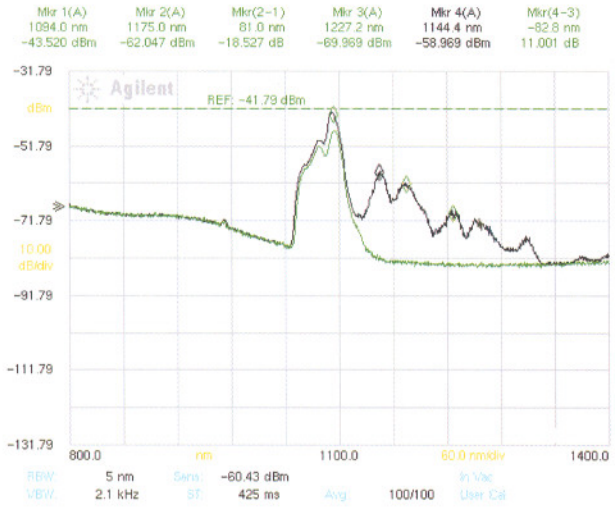

Fig. T.3.6 : Output spectrum in case of low-finesse cavity; the lower trace shows spectrum before onset of random self-pulsing (Pp(0) = 2.5 W), and the upper trace shows spectrum after onset of strong random self-pulsing (Pp(0) = 8 W).-

cavities will respond differently to the distributed backscattered noise in the form of RS and SBS or any other pump-induced noise. Further, weak random self-pulsing in high-finesse resonator with forward- and backward pumping configurations, and strong random self-pulsing in low-finesse cavity shows that highly non-uniform steady-state gain profile with the gain peaking at some point along fiber length, and consequent build-up of random pulse from RS and SBS noise in the case of low-finesse cavity, is essentially responsible for strong random self-pulsing. Thus, to avoid or reduce self-pulsing, it is important to use high-finesse cavity.

Experimental results also show that self-pulsing is initiated as soon as the lasing starts. With increase in pump power, population inversion in the weakly pumped portion also increases and density of atoms in the doped-fiber for signal re-absorption decreases, which results in an increase in initial transmission through the weakly pumped portion and reduction in saturable absorption. The reduction in peak power of self-pulses at higher pump input is also observed experimentally. As the saturable absorption is distributed along the fiber length, period of self-pulsing is random in contrast to regular passively Q-switched output [11,12].

CW fiber laser with fiber Bragg grating mirror:

One of the important advantages of fiber lasers is the provision to use in-line fiber Bragg grating (FBG) mirrors to make it a flexible rugged cavity that is free from misalignments. Use of FBG also provides wavelength selectivity with a narrow linewidth output. Thus, in order to

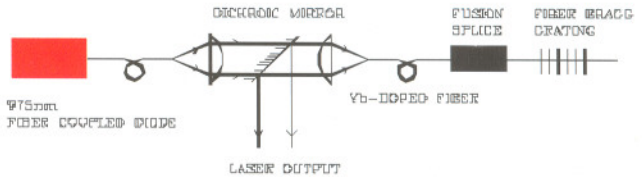

Fig.T.3.7: Experimental set up of the Yb-doped CW fiber laser with fiber Bragg grating mirror.

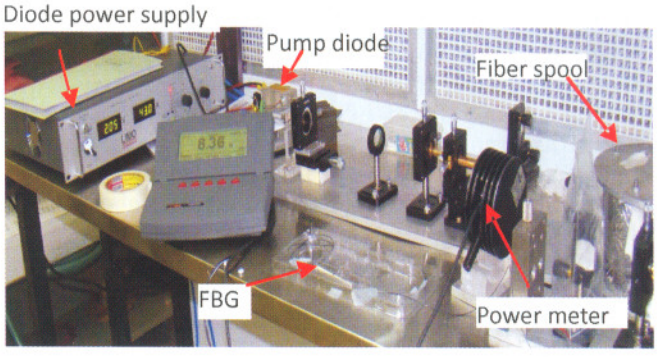

Fig.T.3.8 : A view of the developed Yb-doped CW fiber laser using fiber Bragg grating mirror.

exploit this advantage of Yb-doped fiber laser, and to study the laser output characteristics with narrow band FBG mirror, an experiment to realize Yb-doped CW fiber laser using FBG mirror, written in easily available single-clad fiber, was carried out.

Figure T.3.7 shows a schematic of Yb-doped fiber laser configuration and Fig. T.3.8 shows a view of our bench top Yb-doped CW fiber laser. The experimental set up with FBG mirror comprised of an Yb-doped double clad fiber having a mode field diameter of 10 μm at 1064 nm with NA of 0.075, and an inner clad diameter of 130 μm with NA of 0.46. A 30 W fiber coupled laser diode with center wavelength at 975 nm at 20°C and fiber core diameter of 200 μm was used to pump 2.5 meter length of the Yb-doped fiber. An FBG with ~ 100% reflection at 1093±0.05 nm and FWHM bandwidth of 0.2 nm was spliced at the other fiber end to act as ~ 100% reflecting rear mirror of the Fabry-Perot resonator. This FBG was written in a single mode fiber having MFD at 1060 nm of 6.2±0.3μm. The laser output was taken from the pump fiber end by using a dichroic mirror kept in between the two lenses used for pump coupling. The dichroic mirror is highly transmitting at 975 nm and highly reflecting in a broadband from 1035 nm to 1120 nm, and hence allows the pump wavelength to pass through it and reflect the lasing wavelength.

Fig. T.3.9 shows the output spectrum of the fiber laser having peak lasing wavelength at 1093.18 nm with a narrow FWHM of 0.18 nm. A maximum output power of 8.75 W at an input pump power of 30 W was achieved, with an optical-to-optical conversion efficiency of 29.2%. Low slope efficiency

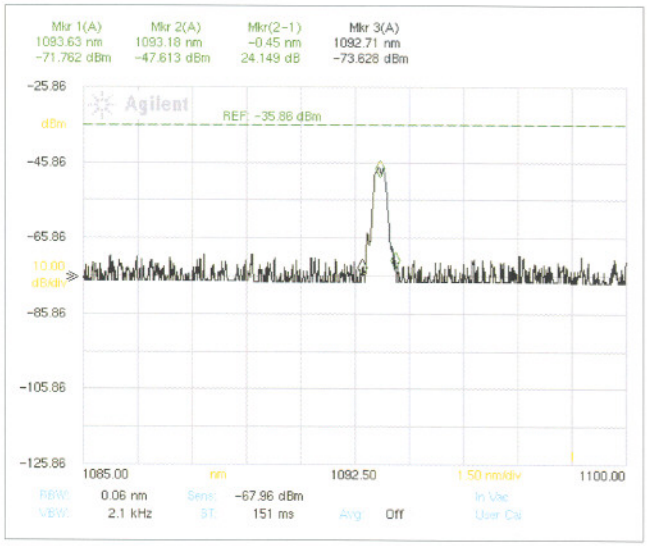

Fig.T.3.9 : Specturm of the ifber laser output peaked at 1093nm with an FWHM of 0.18 nm.

is due to high splice loss because of mismatch of the core MFDs and core NAs between the Bragg grating fiber and the Yb-doped fiber. Efficiency can be further enhanced to reach the maximum reported values of about 80% with improved coupling of pump light and reducing splice loss of Bragg grating fiber with Yb-doped fiber.

Laser output wavelengths peaked at 1030 nm, 1064 nm and 1089 nm with similar efficiencies were also generated by splicing different FBG mirrors with reflection peak at these wavelengths, this shows that Yb-doped fiber gain medium is homogeneously broadened. Thus, tuning over a long wavelength range can be achieved by using a bulk grating or by strain tuning of FBG mirror.

CW fiber laser with double-end pumping:

Figure T.3.10 shows the experimental set-up for double-end pumping of Yb-doped CW fiber laser. It consists of an Yb-doped double-clad fiber of core diameter 10 m with numerical aperture (NA) of 0.075, and an inner-clad diameter of 400 m with a numerical aperture of 0.46. This Yb-doped fiber had an octagonal inner-clad geometry and clad-pump absorption of 0.8 dB/m at 975 nm. Two dichroic mirrors were used in this configuration: one of them has high transmission at 975nm and high reflection in the broad range 1040-1120 nm for normal incidence; the other mirror has similar characteristics at 45 angle of incidence. A maximum output power of 40.5 W was achieved at an input pump power of 58 W, with a slope efficiency of ~ 71.7% and an optical-to-optical conversion efficiency of 69.8%. Threshold pump power for lasing was ~ 1.3 W. Figure T.3.11 shows a view of the in-house developed

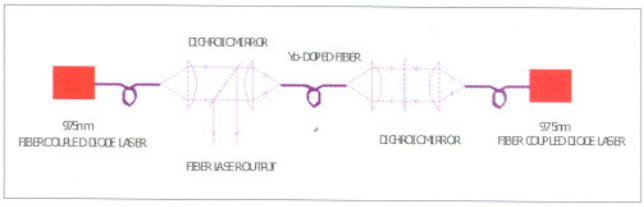

Fig. T.3.10 : Experimental set-up for double -end pumping of an Yb-doped fiber laser.

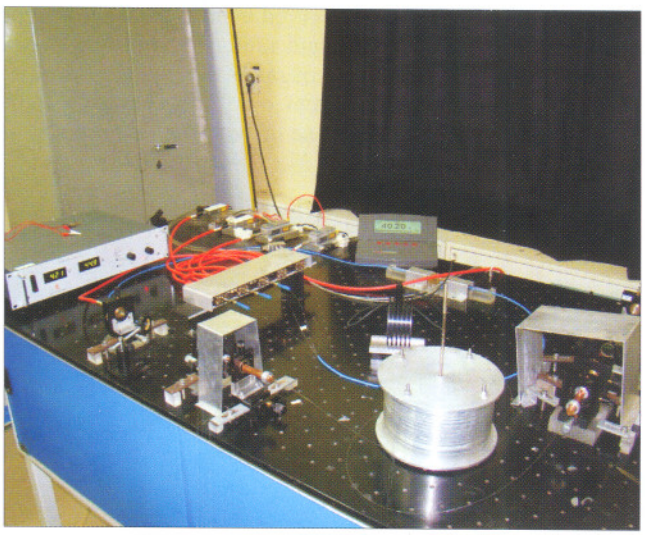

Fig. T.3.11: A view of the in-house developed 40 W Yb-doped CW fiber laser.

bench-top 40 W Yb-doped CW fiber laser. The laser output spectrum was peaked at 1096 nm with a FWHM of ~ 7 nm. The laser output was in single transverse mode with diffraction limited beam quality, and was emitted in a full cone angle of 150 mrad, defined by the NA of the doped fiber[12].

Generation of linearly polarized fiber laser output:

Linearly polarized laser output is required for a variety of applications, such as nonlinear frequency conversion, material processing, spectroscopy, measurements etc. For such applications, linearly polarized Yb-doped fiber lasers are very useful due to their advantages such as diffraction-limited beam quality, high efficiency, intra-core fiber Bragg grating mirrors, compactness and robustness as compared to conventional bulk solid-state lasers. Generation of up to 633 W single-mode plane-polarized Yb-doped CW fiber laser output with about 67% slope efficiency and a polarization extinction ratio of 16 dB, using a multimode fiber of core

diameter 25 μm and bulk polarizing elements has been reported by Jeong et al. [13]. Working of polarization maintaining (PM) fibers is as follows. Optical fibers always exhibit some degree of birefringence, as there is always some amount of residual mechanical stress that is frozen during the fabrication process or other effects which break the circular symmetry. Thus, the state of polarization of light propagating in the fiber gradually evolves along the length of the fiber in an arbitrary fashion due to random bends and stresses in the fiber; in addition, due to changes in ambient conditions, the state of polarization at the exit end of the fiber changes randomly with time. This problem is removed by using a polarization-maintaining (PM) fiber, which is a fiber with a strong built-in linear birefringence. If the polarization of light launched into the fiber is aligned along one of its birefringent axes, this polarization state will be preserved even if the fiber is bent. Working of a PM fiber can be understood in terms of coherent mode coupling. Since the propagation constants of the two polarization modes are different due to the strong in-built birefringence, the relative phase of both the co-propagating modes changes. Thus, any disturbance along the fiber can effectively couple power among the two modes if it has a significant spatial Fourier component with a wave number equal to the difference of the propagation constants of the two polarization modes. If the difference in propagation constants of the two polarization modes is large enough, the normal disturbances in the fiber (such as stresses and bends) which have a very small Fourier component at the required spatial frequency, result in insignificant coupling and thus the polarization state will be preserved. A commonly used method for introducing strong birefringence in a fiber is to include two stress rods, made up of a modified glass composition having a different degree of thermal expansion, in the preform on opposite sides of the core. Stress applying part (SAP) shrinks more than the cladding during the cooling process of fiber drawing, and hence the tensile stress of SAP induces large stress birefringence; this results in different effective mode indices nx and ny for the two orthogonal polarization states. The axis along which the effective mode index is smaller and hence phase velocity is larger is called fast axis; and the axis with the larger mode index is called the slow axis. The modal birefringence depends $B = |n_x - n_y|$ on location and thickness of the SAP. Depending on the shape of fiber cross-section, these are called "PANDA" or "bow-tie" fibers. For a given value of B, the power between the two polarization modes is exchanged periodically as they propagate inside the fiber with the period LB given by

$$L_B = \frac{2\pi}{|\beta_x - \beta_y|} = \frac{\lambda}{B}$$

L_B is referred as the beat length, β_x and β_y are the propagation constants of the modes corresponding to x- and y-polarization states. Figure T.3.11(a) shows geometric cross-section of a PANDA type PM fiber showing its internal structure, and Fig. T.3.11 (b) illustrates the evolution of light polarization along a PM fiber when light is polarized at 45° with respect to the slow and fast axes. In a Yb-doped PANDA-type double-clad PM fiber, the core is doped with Yb_2O_3 and the inner clad contains stress applying parts. Inner-clad is made to have a non-circular shape to avoid excitation of skew modes as in non-PM Yb-doped fibers.

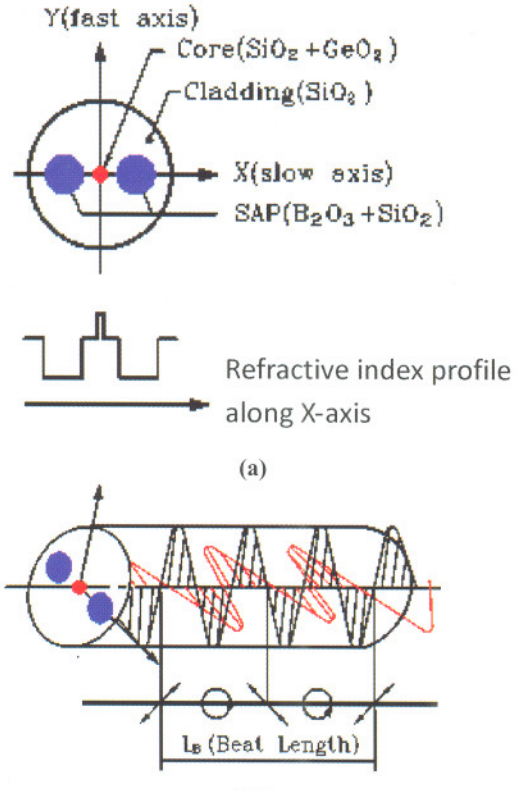

Fig. T.3.11: (a) Geometric cross-section and refractive index profile of a PANDA type of PM fiber, (b) Illustration of evolution of light polarization along the PM fiber when input light is polarized at 45° with respect to the slow and fast axes.

Two experimental configurations, as shown in Fig. T.3.12(a) and T.3.12(b) were studied to generate linearly polarized output. In the experimental set up shown in Fig. T.3.12, a PANDA-type polarization maintaining Yb-doped double-clad fiber having core- and inner-clad diameters of 10μm and 125μm, respectively, was used. Numerical apertures of core and cladding were 0.08 and 0.47 respectively. The two borosilicate stress rods of circular cross section in the inner-clad of the PM fiber resulted in a birefringence of ~ 2.8 x 10^{-4}. The inner clad pump absorption coefficient for this fiber was ~ 2 dB/m at 915 nm. An end-pumping configuration was used to pump the Yb-doped fiber,

which was spooled on a 150 mm diameter aluminum mandrel, to achieve polarized output. A dichroic mirror having high transmission (HT) at 915 nm and high reflection (HR) in the range 1040-1140 nm was placed between the collimating and focusing lenses to transmit the pump beam for end pumping and separate the generated laser output. Another dichroic mirror having HT at 915 nm and HR at 1040-1140 nm was used at the other fiber end for feedback. The laser resonator consisted of a Fabry-Perot cavity with ~ 100% reflectivity at one end (forming the rear mirror) and 4% Fresnel reflection at the cleaved fiber end (forming the output coupler). In the other experimental configuration shown in Fig. T.3.12(b), a polarizer and a λ/2-plate was inserted in the feedback path to ensure feedback along one of the birefringent axis of the PM fiber. In effect, theλ /2-plate does not change the polarization

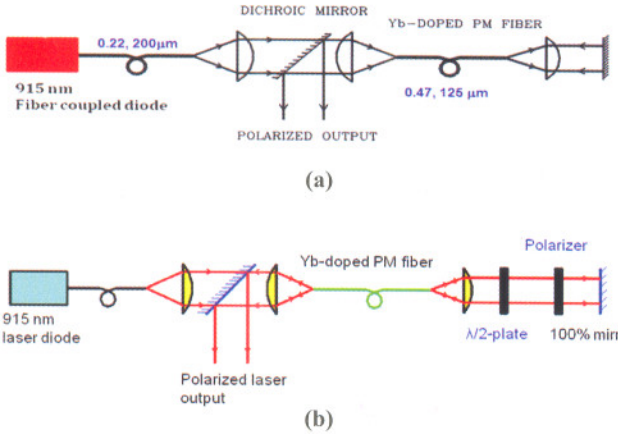

Fig. T.3.12: Schematic of the experimental arrangement of the linearly polarized fiber laser (a) without- and (b) with polarizing element in the feedback path.

after two passes if the beam is polarized just after the right end of the doped fiber, and will not be effective; however, if the beam is unpolarized either due to large spool radius or due to some inhomogeneity in the feedback path, then it can be rotated to provide feedback along one of the birefringent axes and ensure polarized laser output. The output polarization state was confirmed by using a polarizer and analyzer set up in the path of the output laser beam.

Q-switched pulsed fiber laser:

Actively and passively Q-switched fiber lasers with high peak power, high pulse energy and short pulse duration are required for various applications. Among these, actively Q-switched fiber lasers are of interest for applications such as range finding, remote sensing, optical time-domain reflectometry, laser marking, laser surgery and optical parametric oscillator that require short and high peak power pulses. Realization of actively Q-switched multi-moded fiber laser output providing pulse energy as high as 7.7 mJ at 500 Hz repetition frequency and 250 ns pulse duration using a 60 m large core diameter double-clad Yb-doped fiber with $M\sqrt{}^2=7$ has already been reported by Renaud et al.[15]. Single-moded output with a pulse energy of 1.2 mJ at 10 kHz repetition rate and 37 ns pulse duration using a 40 m core diameter fiber has also been reported by Piper et al.[16]. Due to high peak power of the Q-switched pulse that is confined in a fiber core of small cross sectional area and a long fiber cavity, many non-linear effects such as self-phase modulation (SPM), cross-phase modulation (XPM), stimulated Raman scattering (SRS), and stimulated Brillouin scattering (SBS) play a crucial role in their performance [17]. In such Q-switched fiber lasers, SRS could result in the generation of narrower Raman pulses, and transfer of the pulse energy from the lasing signal wave to Raman-Stokes waves. SBS could provide strong feedback to the laser cavity in the form of a short and unstable Brillouin-scattered relaxation pulse. SPM could lead to spectral broadening of the optical pulses and XPM may affect the evolutions of the signal, Brillouin and Raman pulses in the Q-switching process. The small core area of the fiber with a tight mode confinement leads to a high gain for a relatively small amount of energy stored in the gain medium (in the form of excited Yb-ions). The high gain leads to losses via amplified spontaneous emission or even spurious lasing between pulses. This limits the pulse energy that can be stored in the gain medium and thus the energy of the output pulse from a Q-switched fiber laser [18,19].

When a laser beam of frequency is allowed to pass through such an acousto-optic cell at the Bragg angle (which is almost perpendicular to the direction of propagation of the acoustic wave of frequency Ω, diffraction of the beam takes place. The laser beam is diffracted to a single order if the beam is incident at an angle equal to the Bragg angle (θ_B) given by

$$\sin\theta_B = \frac{\lambda_0}{2n_0\Lambda}$$

where n_0 is the refractive index of the medium, λ_0 is the free space optical wavelength and Λ is the acoustic wavelength. Diffracted beam in the +1 order will have a frequency ω+Ω and the diffraction efficiency will depend on acoustic intensity, interaction length and figure of merit of acousto-optic material. When the AO Q-switch is placed inside the laser resonator and RF power is switched on, a fraction of the energy of the laser radiation is diffracted out of the resonator, which results in cavity loss that prevents laser action. When the RF power is switched off, full transmission through the Q-switch cell is restored and a laser pulse is emitted. If the RF power is modulated at a certain repetition rate, laser pulses also get generated at the same repetition rate, and the process is termed as Q-switching.

Figure T.3.13 shows the experimental set-up used in the study of AO Q-switched fiber laser. A 20 W fiber-coupled laser diode emitting at 975 nm was used to pump 18 meters of the Yb-doped double-clad fiber with a core diameter of 10μm and a numerical aperture (NA) of 0.075; the octagonal inner-cladding has a diameter of 400 m with a NA of 0.46, enabling an efficient end-pumping configuration. The laser resonator consists of a Fabry-Perot cavity with a rear mirror of ~ 100% reflectivity, and 4% Fresnel reflection at the other cleaved end, which forms the output coupler. A dichroic mirror, which is highly transmitting at 975 nm and highly reflecting in the wavelength band from 1064 nm to 1140 nm was used to couple out the Q-switched laser beam. To achieve faithful Q-switching operation, one of the fiber ends has been angle-polished at 10^0 to prevent any feedback that could result in spurious lasing between the pulses. The AO switch operated at a radio frequency of 27.12 MHz with modulation rate 1 kHz-100 kHz, and variable duty cycle was applied in the study of Q-switching action. The AO modulator, which was kept near the rear mirror end, provides a diffraction efficiency of about

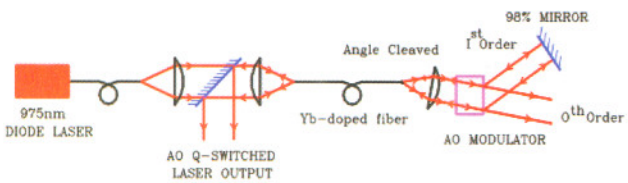

Fig.T.3.13: Experimental set-up to study Q-switched fiber laser.

60% with a deflection angle of 7.68 mrad. With RF modulation, the first order beam is either fully present or absent and therefore a faithful Q-switching is achieved with first order diffracted beam. At the maximum pump power of 17.2 W, stable pulses were achieved in the modulation range 15 kHz-100 kHz. At lower repetition rates, i.e. in the range 1-15 kHz, it was required to sufficiently lower the pump power to achieve stable pulses. Fig. T.3.14 shows the measured pulse energy and pulse width as a function of modulation frequency. A maximum pulse energy of 285 μJ was achieved with a pulse duration of 220 ns at 15 kHz modulation frequency [20].

Observation of single and multi-pulse output:

We first studied the effect of AO Q-switch ON- and OFF-timings on the output pulse shape. In this study, for a typical modulation frequency of 20 kHz, with 22 s modulator OFF-time and 17.12 W pump power, we obtained a maximum average output power of 4.5 W, with a single un-modulated pulse of 225μJ pulse energy and 240 ns full-width at half-maximum (FWHM) pulse duration. Figures T.3.15(a)-(d) shows typical multi-pulse appearance in the output at 20 kHz modulation frequency. The pump power was 11.72 W. The

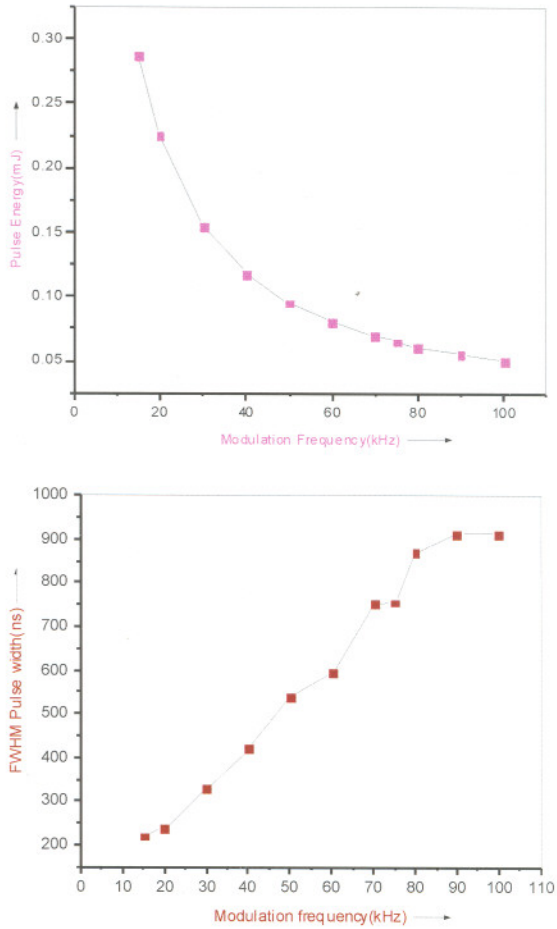

Fig. T.3.14: Measured pulse energy and FWHM pulse width as a function of modulation frequency.

number of post pulses in the output decreases with increase in the modulator OFF-time. When the modulator OFF-time was increased from 5.2 μs to 32μ s, number of post pulses reduced from five to nil. Pulse build-up time of the principal pulse also decreases with increase in modulator OFF-time; the peak power of the principal pulse increases with reduction in the number of post pulses, and finally a desired single pulse output is observed. When the modulator OFF-time was further increased, the amplitude stability of the principal pulse became poor.

When the modulator OFF-time (i.e. low Q) is large enough, population inversion and hence gain builds up in the system. A large initial gain facilitates the formation of a single Q-switched pulse (Fig.T.3.15d). As the modulator OFF-time is reduced considerably, the initial gain available for pulse build-up is reduced and full energy extraction may not be possible. As a result smaller satellite pulses are also generated. Thus, for very small modulator OFF-timings, the additional

available gain is so small that the normal Q-switching process is disturbed, and the laser output breaks into relaxation oscillations as shown in Fig. T.3.14(a)-(c). In this case multiple pulses are observed with a pulse separation of about 10-12μ s, which can be understood by considering a slight loss-modulation in the cavity and the resultant fluctuation of population inversion. Since the pulse build-up time also depends on initial gain, one can see the reduction in the pulse build-up time from 5.2μs to 3.88μs as the modulator OFF-time is increased from 5.2μs to 32μs. As it is possible to increase the gain in the system by using higher pump powers, reduction in pulse build-up time can be easily achieved. Indeed, as the pump power and hence gain increases, the modulator OFF-time could be considerably reduced before the laser output changes from a single pulse to multiple pulses due to relaxation oscillations, which is expected. As the modulator OFF-time is increased beyond a certain optimum limit, probably the large gain in the system causes ASE generation, which leads to amplitude fluctuations in the Q-switched output. This shows that for a given pump power, there is an optimum value for the modulator OFF-time to generate a stable single pulse output in Q-switched fiber lasers.

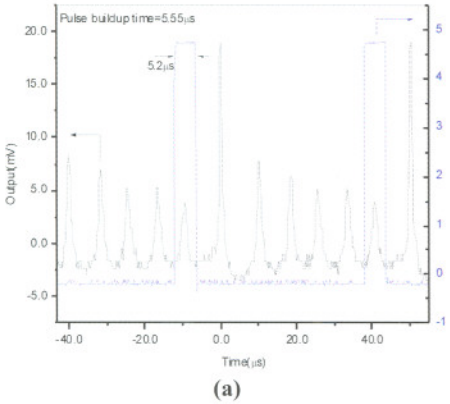

(a)

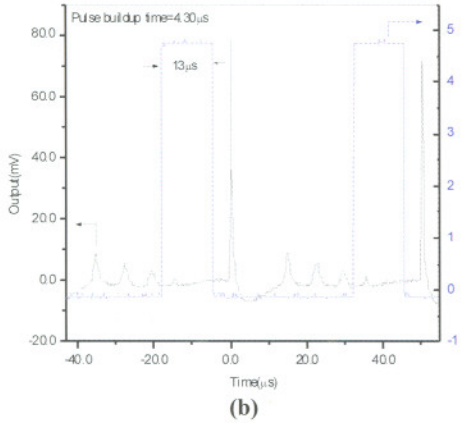

(b)

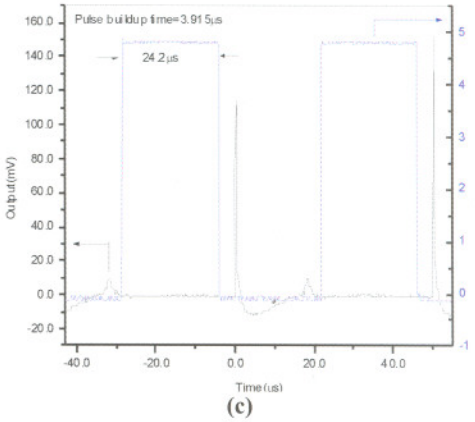

(c)

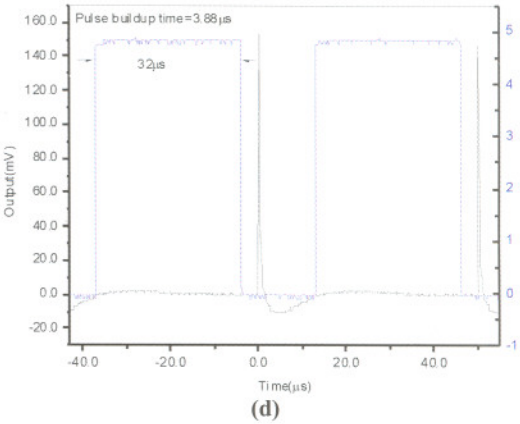

(d)

Fig.T.3.15 : (a)-(d) Observation of multi-pulses and disappearance of post pulses with increasing modulator OFF-time in the output of the Q-switched Yb-doped fiber laser at a typical modulation frequency of 20 kHz and a fixed input pump power of 11.72 W; blue trace shows modulating signal and black trace shows output laser pulses.

Observation of 'mode-locked resembling' pulse output:

Experiments were also carried out to observe mode-locked resembling pulse output. In literature, Myslinski et al.[21,22] have observed periodic modulation within the Q-switched envelope, which was attributed to 'simultaneous Q-switching and mode-locking' in AO Q-switched fiber laser due to SPM. It was also stated that these periodic modulations appeared only after a careful adjustment of the mirror. We were able to reproduce similar pulse shapes by carefully adjusting the position of mirror near the AOM. Figure T.3.16(a) shows a periodically modulated mode-locked resembling pulse shape at 32 kHz modulation frequency and input pump power of 12 W. The FWHM pulse width of the Q-switched envelope is 260 ns, with an average output power of 3.2 W. One can note that the separation between individual pulses within the Q-switched envelope is about 18-20 ns (pulse repetition frequency of about 50 MHz), which is much

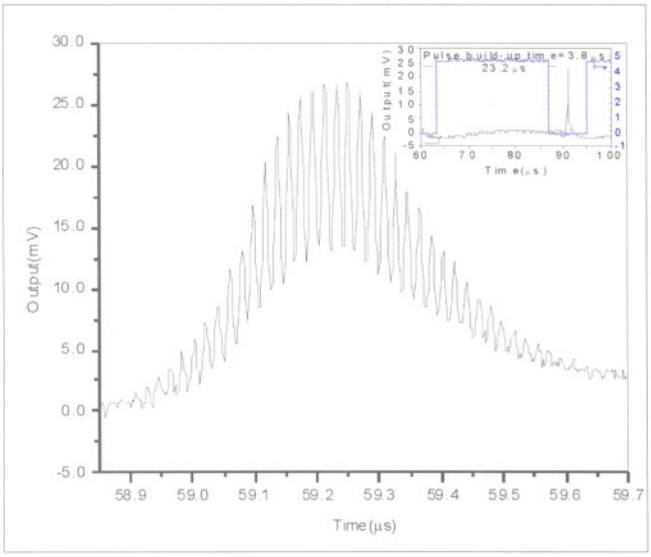

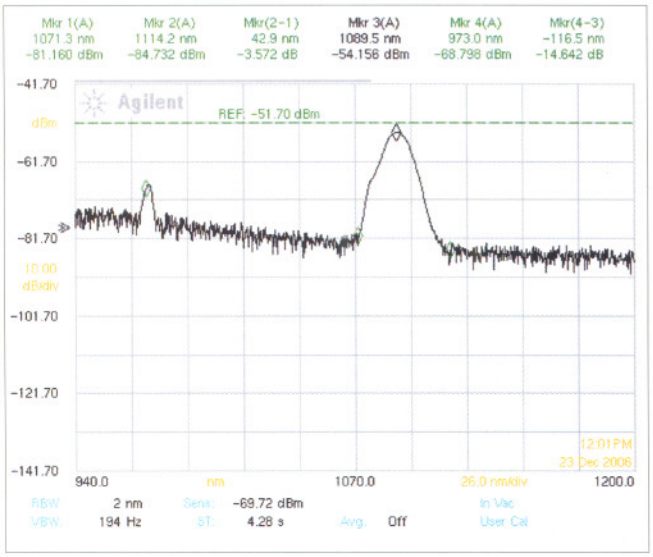

Fig.T.3.16 : (a) Mode-locked resembling pulse shape, and (b) the corresponding output spectrum at 32 kHz modulation frequency and at an input pump power of 12 W. Inset shows modulating signal with a modulation window ON-time of t_{ON} = 23.2μs (blue trace) and 'mode-locked resembling pulse' with a delay equal to the pulse build-up time (black trace).

smaller than the cavity round-trip time of 174 ns, corresponding to a cavity mode spacing of 5.75 MHz. Thus, the pulse repetition frequency of 50 MHz is neither equal to cavity mode spacing nor equal to its harmonics, as one would expect in the case of mode-locking a laser. The pulse width of the individual pulses within the envelope was about 8 ns. It was also observed that the modulation depth of 'mode-locked resembling' pulse can be increased or decreased, when the modulation window ON-time and mirror alignment is adjusted carefully. Figure T.3.16(b) shows the output spectrum corresponding to the pulse in Fig. T.3.16(a). The recorded pulse band-width of 42.9 nm corresponds to about 100 fs mode-locked pulses in contrast to the observed pulse duration of 8 ns.

Here, we have shown that the mode-locked resembling periodic modulation of Q-switched envelope is due to mode beating between the zeroeth order and the first order (frequency shifted) diffracted beams from the AOM. As stated earlier, the periodic modulation could be obtained by 'carefully adjusting the rear mirror position'. We then systematically recorded the output pulse as the highly reflecting rear mirror was moved closer to and farther away from the AOM. When the rear mirror was far away (~ 0.5 m) from the AOM, the output pulse was smooth without any modulation. When the mirror was brought nearer (~ 0.1 m) to the AOM, periodic modulation appeared in the Q-switched envelope on adjustment of the modulation window ON-time and the mirror tilt. The 'mode-locked resembling' periodic modulation of the pulse envelope was also observed at 20, 24, 27 & 30 kHz modulation frequencies. If ω and Ω are the frequencies of laser and radio frequencies (RF) applied to the AO cell, the first order diffracted beam will have a frequency $\omega + \Omega$. After feedback it passes again through the AO cell and gets diffracted again to give $\omega+2\Omega$ in the first order, in a direction in which the laser beam was propagating before operation of the Q-switch. Now, the two signals at and $\omega+2\Omega$ will give a mode beat at 2Ω with a maximum modulation depth if both signals have similar intensities. On observation of the mode-locked resembling Q-switched pulses obtained in our experiment, we found that the separation between individual pulses within the Q-switched envelope is about 18-20 ns (measurement limited by detection system), which corresponds to mode beat at 50-55.5 MHz. The RF wave applied to the Q-switch in our case was 27.12 MHz, which corresponds to 2Ω = 54.24 MHz, and matches very well with the observed beat frequency. As the angular separation between the zeroeth and the first order (frequency shifted) diffracted beams are rather small, such a mixing of zeroeth order and first order diffracted beams can occur only when the mirror is close to the Q-switch, which was otherwise meant for providing feedback using the first order diffracted beam. Further, in our experiments, we could change the modulation depth by changing the ratio of feedback from the first and the zeroth order beams by means of slight adjustment of the mirror alignment. This further confirms the proposition of mode-beating. Thus, our experimental observations, as well as observations by Myslinski et al. [22], could be explained with the above proposition. This identifies the physical phenomenon responsible for the occurrence of mode-locked resembling pulses within the Q-switched pulse envelope, and is attributed to mode-beating between the round-trip

frequency-shifted beam at $\omega+2\Omega$ and the original (un-deviated) beam at ω.

Acknowledgements:

This work has been carried out as a part of Ph. D. thesis. Author would like thank his supervisors Prof. K. Thyagarajan and Prof. M. R. Shenoy from IIT Delhi for their invaluable guidance throughout this work. The author also wishes to acknowledge Dr. S. M. Oak for his constant support and suggestions during this work. Author also acknowledges all the members of SSLD for their help from time to time during this work.

References:

1. Y. Jeong et.al., Opt. Express 12, pp. 6088-6092 (2004).
2. http//www.ipgphotonics.com
3. H. M. Pask et.al., IEEE J. Selected Topics in Quantum Electronics 1, pp. 2-13 (1995).
4. F. Brunet et.al., J. Lightwave Technol. 23, pp. 2131-2138 (2005).
5. B. Ortac et.al., Opt. Commun. 215, pp. 389-395 (2003).
6. A. Hideur et.al., Opt. Commun. 186, pp. 311-317 (2000).
7. P. Glas, Opt. Commun. 161, pp. 345-358 (1999).
8. Suzuki, A., et.al. IEEE Photonics Technol. Lett., 19, pp. 1463-1465 (2007).
9. Guan, W., and Marciante, J. R., "Complete elimination of self-pulsations in dual-clad ytterbium-doped fiber lasers at all pumping levels", Opt. Lett. 34, pp. 815-817 (2009).
10. B. N. Upadhyaya et.al., "Effect of steady-state conditions on self-pulsing characteristics of Yb-doped cw fiber lasers", Opt. Commun. 281, pp. 146-153 (2008).
11. B. N. Upadhyaya et.al., "Self-pulsing characteristics of a high-power single transverse mode Yb-doped CW fiber laser", Opt. Commun. 283, pp. 2206-2213 (2010).
12. B. N. Upadhyaya et.al., "Effect of laser linewidth and fiber length on self-pulsing dynamics and output stabilization of single-mode Yb-doped double-clad fiber laser", Appl. Opt. 49, pp. 2316-2325 (2010).
13. Y. Jeong et.al., "Single-mode plane-polarized ytterbium-doped large-core fiber laser with 633 W continuous-wave output power" Opt. Lett. 30, pp. 955-957 (2005).
14. B. N. Upadhyaya et.al. "International Conference on Optoelectronics, Fiber Optics and Photonics: PHOTONICS-2008, pp. 286, IIT Delhi, New Delhi, India, Dec. 13-17, 2008.
15. C. C. Renaud, et.al., Conference on Lasers and Electro-optics, Technical Digest, Baltimore, pp. 219, CTuQ5, MD, USA, 6-11 May 2001.
16. A. Piper et.al., CLEO 2003, vol.1, pp. 2, 16-21 May 2004.
17. G. P. Agrawal, Nonlinear Fiber Optics, Second ed., Academic Press, San Diego, 1995.
18. C. C. Renaud et.al., IEEE J. Quantum Electron. 37, pp. 199-206 (2001).
19. Y. Wang, and C. Q. Xu, IEEE J. Quantum Electron. 40, pp. 1583-1596 (2004).
20. B. N. Upadhyaya et.al., International Conference on Optoelectronics, Fiber Optics and Photonics: Photonics-2006, WeB 12, pp. 23, Hyderabad, India, Dec. 13-16, 2006.
21. P. Myslinski et.al., Appl. Opt. 32, pp. 286-290 (1993).
22. P. Myslinski, et.al. IEEE J. Quantum. Electron. 28, pp. 371-377 (1992).
23. B. N. Upadhyaya et.al., Opt. Exp. 15, pp. 11576-11588 (2007).